Met. Mater. Int., Vol. 16, No. 6 (2010), pp. 891~894
doi: 10.1007/s12540-010-1206-1 Published 27 December 2010

Effect of Hot-Forging on Mechanical Properties of Silicon Carbide Sintered with Al_2O_3-Y_2O_3-MgO

Myong-Hoon Roh[1], Wonjoong Kim[1,*], Young-Wook Kim[1], and Min-Hyung Choi[2]

[1]Department of Materials Science and Engineering, the University of Seoul, Seoul 130-743, Korea
[2]Department of Computer Science and Engineering, University of Colorado at Denver, Denver, CO 80207, USA

(received date: 5 October 2009 / accepted date: 8 September 2010)

The mechanical properties of hot-pressed and hot-forged SiC were investigated. The hot -forging of the hot-pressed SiC was carried out at 1700 °C for 66 h under an applied pressure of 25 MPa in an argon atmosphere. The microstructures on the surfaces parallel and perpendicular to the pressing direction of the hot-pressed and hot-forged SiC were similar, and no texture development was observed because of the lack of massive $\beta \rightarrow \alpha$ transformation of SiC. An increase in hardness of about 13 % and fracture toughness of about 33 % was achieved in the hot-forged specimens compared to the hot-pressed specimens.

Keywords: deformation, microstructure, phase transformation, toughness, hardness

1. INTRODUCTION

Silicon carbide is one of the most widely used non-oxide ceramics. Its high hardness and chemical inertness make it useful as a wear-resistant material, while its strength retention and resistance to oxidation and thermal shock make it attractive in structural applications at elevated temperatures [1-5]. The superplasticity of SiC was discovered in liquid-phase-sintered SiC with a grain size of 90 nm fabricated by hot -pressing in 1995 [6] and in solid-state-sintered SiC with a grain size of 200 nm fabricated by ultrahigh-pressure hot – isostatic -pressing in 1998 [7]. Grain-boundary sliding was found to be the main mechanism of the superplasticity in SiC ceramics [6-8]. It is well documented that boron segregation at the grain boundaries promotes grain-boundary sliding in solid-state-sintered SiC [9], and the presence of a stable glassy phase at elevated temperatures is the key to improving the superplasticity of liquid-phase-sintered SiC [8,10,11]. Generally, SiC ceramics with nano-sized grains are superplastic at elevated temperatures [6-8]. However, there have been few reports on the texture development and mechanical properties of hot-forged SiC ceramics with micron-sized grains. Kim *et al.* [12] produced a textured α-SiC specimen by annealing as-hot-pressed α-SiC and reported the texture formation mechanism to be phase-transformation-induced anisotropic grain growth [12]. Sacks *et al.* [13] applied a template grain growth approach to develop a highly textured α-SiC specimen. The seeded α-SiC with a preferred orientation grew anisotropically, but at the expense of small non-oriented matrix grains. Xie *et al.* [14] also developed textured SiC ceramics by hot -forging a hot-pressed SiC specimen at 1900 °C for 4 h under a constant pressure of 25 MPa. Grain rotation during hot forging was suggested as a possible mechanism for texture development. Lee *et al.* [15] developed SiC ceramics with an anisotropic microstructure by hot forging a hot-pressed SiC specimen at 1900 °C for 4 h under a constant pressure of 25 MPa. The anisotropic microstructure was developed by the $\beta \rightarrow \alpha$ transformation of SiC during hot forging. They observed strengthening and hardening in the surface perpendicular to the hot-forging direction and toughening in the surface parallel to the hot-forging direction.

All the previous studies on hot-forged SiC discussed the occurrence of the appreciable $\beta \rightarrow \alpha$ phase transformation of SiC during hot -forging. The mechanical properties of hot-forged SiC without phase transformation or with minimal phase transformation have not been investigated yet. In this study, to suppress or minimize the phase transformation of SiC during hot -forging, a hot-pressed SiC specimen was hot -forged at a temperature as low as 1700 °C under a constant pressure of 25 MPa, and the effect of hot -forging on the mechanical properties of the hot-pressed SiC ceramic without phase transformation or with minimal the phase transformation was investigated.

*Corresponding author: wjkim@uos.ac.kr

2. EXPERIMENTAL PROCEDURE

Commercially available β-SiC (Ultrafine, Ibiden Co., Ltd, Nagoya, Japan), Al_2O_3 (AKP30, Sumitomo Chemical Co., Tokyo, Japan), Y_2O_3 (Grade fine, H. C. Stark, Germany), and MgO (99.9 %, High Purity Chemicals, Japan) were used as the starting materials. The mean particle size and specific surface area of the β-SiC powder were 0.27 μm and 23.3 m^2/g, respectively. A combination of 90 wt.% β-SiC, 7 wt.% Al_2O_3, 2 wt.% Y_2O_3, and 1 wt.% MgO was ball-milled in ethanol for 24 h using SiC balls. The mixed slurry was dried, sieved through a 60-mesh screen, and then hot -pressed at 1750 °C for 1 h under a pressure of 25 MPa in an argon atmosphere. The hot-pressed specimen was cut into 20 mm × 17 mm × 9 mm pieces and hot-forged at 1700 °C for 66 h under a pressure of 25 MPa in an argon atmosphere.

The relative densities of the hot-pressed and hot-forged specimens were measured using the Archimedes' method. The theoretical density of the specimens was calculated according to the rule of mixtures. The hot-pressed and hot-forged specimens were cut, polished, and then etched by a CF_4 plasma containing 20 % O_2. The microstructures were observed using scanning electron microscopy (SEM). The phase identification of the hot-pressed and hot-forged specimens was carried out by X-ray diffraction (XRD) with Cu Kα radiation. The Vickers hardness was measured using a Vickers indenter under a load of 4.9 N on the surfaces parallel (designated as surface P) and perpendicular (surface T) to the hot-pressing direction. The fracture toughness was determined by measuring the crack lengths that were generated by a Vickers indenter with a load of 98 N on surfaces P and T [16].

3. RESULTS AND DISCUSSION

The thickness and reduction rate of the hot-forged specimen were 6.24 mm and 30 %, respectively. The hot- forging of SiC was performed at an initial strain rate of -8.4×10^{-5} s^{-1} for 30 h. The specimen was further deformed at a much lower strain rate of -1.8×10^{-5} s^{-1} after 30 h.

The relative densities and processing parameters of the hot-pressed SiC (HPSC) and hot-forged SiC (HFSC) are shown in Table 1. As shown in Table 1, the relative density of SiC increased from 97.7 % to 99.2 % after hot -forging. The increase in the relative density of SiC resulted from the removal of the residual pores caused by grain-boundary sliding (GBS) during hot -forging [8].

Table 1. Relative densities and phase of SiC ceramics investigated

Specimen	Processing	Relative density (%)	Phase	
			Major	Trace
HPSC	1750/1 h/25 MPa/Ar	97.7	β-SiC	-
HFSC	1700/66 h/25 MPa/Ar	99.2	β-SiC	α-SiC

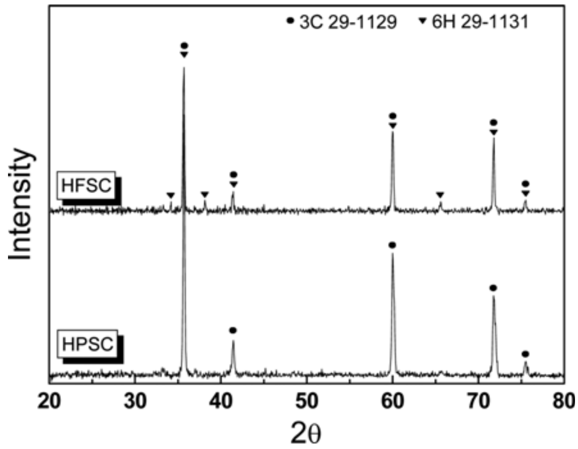

Fig. 1. XRD patterns of the hot-pressed (HPSC) and hot-forged (HFSC) specimens.

The XRD patterns of HPSC and HFSC are shown in Fig. 1. The major phase in both the hot-pressed and hot-forged specimens was β-SiC (3C), and no peak corresponding to the sintering additives was observed. In the hot-forged specimen, a trace of α-SiC (6H) was observed. To compare the texture development of the hot-pressed and hot-forged specimens, we measured their pole-figures by the Schultz reflection method and Cu Kα radiation using a pole-figure goniometer. Neither specimen showed any texture development. This result was consistent with the microstructure observation (Fig. 2). In Fig. 2, SiC grains are etched away by the CF_4 plasma, so that the microstructures are delineated by the grain-boundary glassy phase. It was observed that the microstructures taken from surfaces P and T of the hot-pressed (Figs. 2(a) and (b)) and hot-forged (Figs. 2(c) and (d)) specimens were similar, i.e. a random microstructure. The hot-pressed specimen features a dense, equiaxed microstructure consisting of β-SiC grains and the secondary Si-

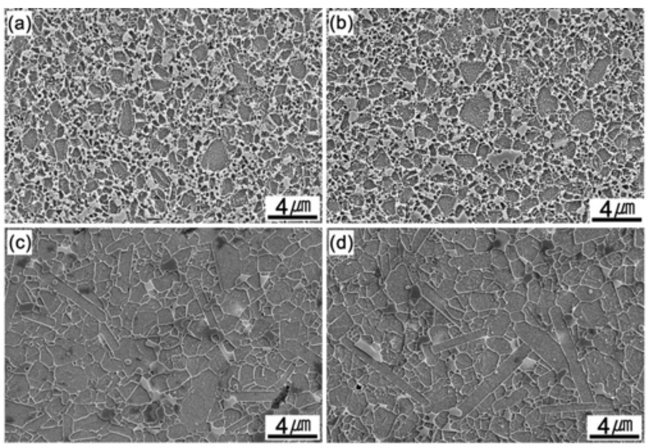

Fig. 2. Typical microstructures of the as-hot-pressed (HPSC) and hot-forged (HFSC) specimens: (a) HPSC(P), (b) HPSC(T), (c) HFSC(P), and (d) HFSC(T) (refer to Table 1).

Mg-Al-Y-O-C glassy phase. The grains of the hot-pressed specimens were fully wetted. The microstructure of the hot-forged specimen consisted mainly of equiaxed grains and partially elongated grains. Glassy phase junctions were also observed. As the elongated SiC grains are composed of α-SiC (6H), they correspond to the crystalline peaks of α-SiC observed in the XRD pattern (Fig. 1). Although a small amount of phase transformation was observed in the hot-forged specimen, the major phase of this specimen was β-SiC (3C). Most of the SiC grains retained their equiaxed shape when grain growth occurred during the hot -forging at 1700 °C for 66 h. Therefore, grain-boundary sliding is the major mechanism of the plastic deformation of the hot-forged material. The reason for the lowering of the strain rate with increasing hot-forging time, as mentioned above, was the dynamic grain growth of equiaxed grains and the growth of elongated grains during hot-forging [6].

The amount of second phase in the hot-forged SiC (Fig. 2(c) and (d)) was observed to be smaller that that in as-hot-pressed SiC (Fig. 2(a) and (b)). This is due to the weight loss (~4.29 %) which took place during hot -forging. The weight loss is attributed to the volatilization of a liquid phase formed from the sintering additives (Al_2O_3-Y_2O_3-MgO).

Figure 3 shows the variation of the Vickers hardness values obtained from surfaces P and T. The hardness values of the hot-pressed specimens obtained from surfaces P and T were 21.4 GPa and 21.6 GPa, respectively, and those of the hot-forged specimens were 24.3 GPa and 24.5 GPa, respectively. As shown in Fig. 2, the microstructures of surfaces P and T for the hot-pressed and hot-forged SiC were similar; therefore, there was no difference in the hardness values at these surfaces. However, the hardness of the hot-forged specimen was higher than that of the hot-pressed specimen. The increased hardness value (~13 %) of the hot-forged specimen resulted from its increased relative density and partly reduced grain-boundary phases (second phase) originating from the sintering additives. Also, the Vickers hardness of SiC (25 GPa to 34 GPa) is generally higher than that of the grain-boundary phases (in the case of Al_2O_3-Y_2O_3, ~15 GPa). Therefore, the hardness value of the hot-forged specimen increased after hot -forging because the probability of indentation into SiC grains grown by the Ostwald ripening mechanism was higher than that of the hot-pressed specimen fully wetted by grain-boundary phases which had a lower hardness value [17].

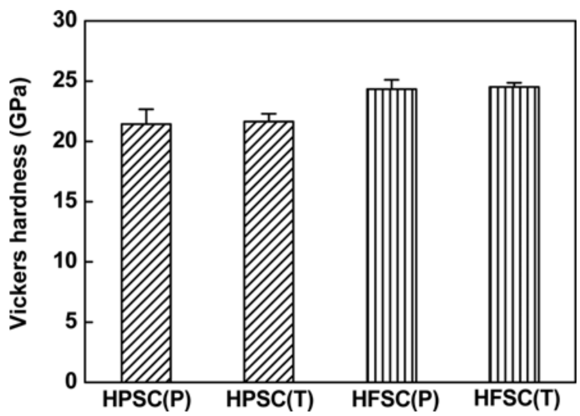

Fig. 3. Vickers hardnesses of the hot-pressed (HPSC) and hot-forged (HFSC) specimens.

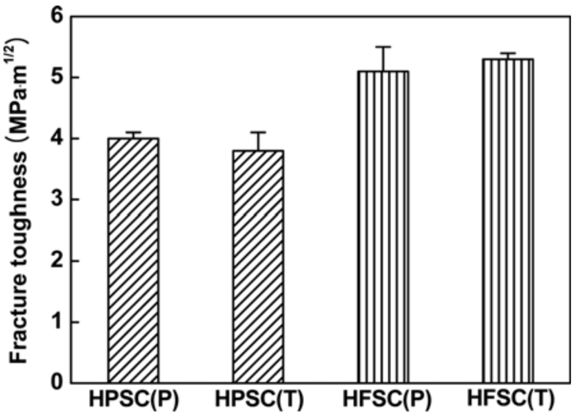

Fig. 4. Fracture toughnesses of the hot-pressed (HPSC) and hot-forged (HFSC) specimens.

Figure 4 shows the variation of the toughness values obtained from surfaces P and T. The toughness values of the hot-pressed specimens obtained from surfaces P and T were 4.0 MPa·m$^{1/2}$ and 3.8 MPa·m$^{1/2}$, respectively, and those of the hot-forged specimens were 5.1 MPa·m$^{1/2}$ and 5.3 MPa·m$^{1/2}$, respectively. Because the microstructures of surfaces P and T of the hot-pressed and hot-forged SiC were similar, there was no difference in the toughness values at these surfaces. However, the toughness of the hot-forged specimen, which had a bimodal microstructure composed of equiaxed and elongated grains, was about 33 % higher than that of the hot-pressed specimen. The increase in the fracture toughness was mainly attributed to crack deflection and possibly also to bridging by the elongated grains in the hot-forged specimen [5]. As shown in Fig. 5, the crack propagation in the hot-forged specimen was more tortuous than the other, showing crack deflection as the operating mechanism for the toughening.

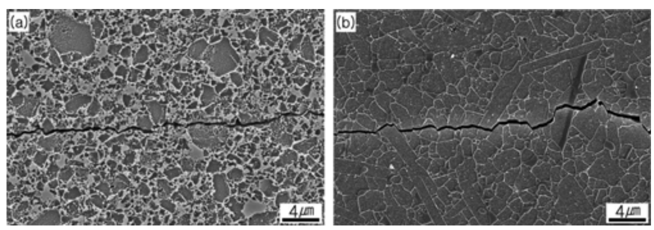

Fig. 5. SEM images of the cracks (produced by Vickers indentation) in hot-pressed (HPSC) and hot-forged (HFSC) specimen: (a) HPSC and (b) HFSC.

4. CONCLUSION

Hot-pressed SiC with Al_2O_3, Y_2O_3, and MgO as sintering additives was hot -forged at 1700 for 66 h under a constant pressure of 25 MPa in an argon atmosphere. The hot-forging increased the relative density of SiC from 97.7 % to 99.2 %. During hot-forging, both grain growth and partial phase transformation of the equiaxed grains took place and the microstructure changed from an equiaxed to a bimodal microstructure consisting mostly of equiaxed grains and a small number of elongated grains. The strain rate of the hot-forged SiC decreased with increasing hot-forging time. It was observed that the microstructures taken from surfaces P and T of both the hot-pressed and hot-forged specimens were similar. Therefore, no difference in the hardness and toughness values at surfaces P and T was found. A 13 % increase in hardness (21.5 GPa 24.4 GPa) was achieved in the hot-forged specimens compared to the hot-pressed specimens because of the increased densification and grain growth which took place during hot -forging. A 33 % increase of the fracture toughness (3.9 $MPa.m^{1/2}$ 5.2 $MPa.m^{1/2}$) in the hot-forged specimens was mainly attributed to crack deflection and possibly also to bridging by the elongated grains in the hot-forged specimens.

ACKNOWLEDGMENT

This work was supported by a Research Grant from the University of Seoul in 2007.

REFERENCES

1. A. M. Kueck, D. K. Kim, Q. M. Ramasse, L. C. D. Jonghe, and R. O. Ritchie, *Nano Lett*. **8**, 2935 (2008).
2. D. A. Ray, S. Kaur, R. A. Cutler, and S. K. Shetty, *J. Am. Ceram. Soc*. **91**, 2163 (2008).
3. Y.-W. Kim, Y. S. Chun, T. Nishimura, M. Mitomo, and Y. H. Lee, *Acta mater*. **55**, 727 (2007).
4. K. Y. Lim, D. H. Jang, Y.-W. Kim, J. Y. Park, and D. S. Park, *Met. Mater. Int*. **14**, 589 (2008).
5. S. I. Ko, S. J. Lee, M. H. Roh, W. Kim, and Y.-W. Kim, *Met. Mater. Int*. **15**, 149 (2009).
6. M. Mitomo, Y.-W. Kim, and H. Hirotsuru, *J. Mater. Res*. **11**, 1601 (1996).
7. Y. Shinoda, T. Nagano, H. Gu, and F. Wakai, *J. Am. Ceram. Soc*. **82**, 2916 (1999).
8. T. Nagano, K. Kaneko, G. D. Zhan, M. Mitomo, and Y.-W. Kim, *J. Europ. Ceram. Soc*., **22**, 263 (2002).
9. H. Gu, Y. Shinoda, and F. Wakai, *J. Am. Ceram. Soc*., **82**, 469 (1999).
10. T. Nagano, H. Gu, K. Kaneko, G. D. Zhan, and M. Mitomo, *J. Am. Ceram. Soc*., **84**, 2045 (2001).
11. Y. I. Lee, Y.-W. Kim, and M. Mitomo, *J. Mater. Sci*. **39**, 3613 (2004).
12. W. Kim, Y.-W. Kim, and D. H. Cho, *J. Am. Ceram. Soc*. **81**, 1669 (1998).
13. M. D. Sacks, G. W. Scheiffele, and G. A. Staab, *J. Am. Ceram. Soc*. **79**, 1611 (1996).
14. R. J. Xie, M. Mitomo, W. Kim, Y.-W. Kim, G. D. Zhan, and Y. Akimune, J. *Am, Ceram. Soc.* **85**, 459 (2002).
15. S. H. Lee, Y. I. Lee, Y.-W. Kim, R. J. Xie, M. Mitomo, and G. D. Zhan, *Scripta mater*. **52**, 153 (2005).
16. G. R. Anstis, P. Chantikul, B. R. Lawn, and D. B. Marshall, *J. Am. Ceram. Soc*. **64**, 533 (1981).
17. Borrero-Lopez, A. Pajares, A. L. Ortiz, and F. Guiberteau, *J. Europ. Ceram Soc*. **27**, 3359 (2007).